Project title:	Combined thermal and visual image analysis for crop scanning and crop disease monitoring
Project number:	CP60a
Project leader:	Dr. Nasir Rajpoot
Report:	Annual report, July 2012
Previous report:	
Key staff:	Shan-e-Ahmed Raza Dr. Nasir Rajpoot Dr. John Clarkson
Location of project:	University of Warwick
Industry Representative:	Alan Davis
Date project commenced:	11 March 2011
Date project completed (or expected completion date):	10 March 2014

DISCLAIMER

AHDB, operating through its HDC division seeks to ensure that the information contained within this document is accurate at the time of printing. No warranty is given in respect thereof and, to the maximum extent permitted by law the Agriculture and Horticulture Development Board accepts no liability for loss, damage or injury howsoever caused (including that caused by negligence) or suffered directly or indirectly in relation to information and opinions contained in or omitted from this document.

[The results and conclusions in this report are based on an investigation conducted over a one-year period. The conditions under which the experiments were carried out and the results have been reported in detail and with accuracy. However, because of the biological nature of the work it must be borne in mind that different circumstances and conditions could produce different results. Therefore, care must be taken with interpretation of the results, especially if they are used as the basis for commercial product recommendations.]

AUTHENTICATION

We declare that this work was done under our supervision according to the procedures described herein and that the report represents a true and accurate record of the results obtained.

Dr. Nasir Rajpoot
Associate Professor
University of Warwick

Signature ..... Date .....

Dr. John Clarkson
Research Scientist
University of Warwick

Signature ..... Date .....

Report authorised by:

[Name]
[Position]
[Organisation]

Signature ..... Date .....

[Name]
[Position]
[Organisation]

Signature ..... Date .....

CONTENTS

GROWER SUMMARY

Headline

New software is under development to create an accurate 3D thermal profile of a crop with the aim of accurately identifying temperature anomalies associated with plant stress. Early developments using data from water stress treatments indicate the potential for this approach.

Background

Infrared thermometers have been used since the early 80's to determine the temperature differences in plants and different parts of canopy by researchers for irrigation scheduling purposes. However, the development of thermal imaging cameras has extended the opportunities for more detailed and sensitive analysis of the thermal properties of plants and canopies. This has led to the development of different applications including early detection of water stress, plant disease and plant phenotyping. One of the major problems associated with thermal imaging in plants is temperature variation due to canopy architecture and other external factors. Leaf angles, sunlit and shaded regions, environmental conditions and the distance of the plant from the camera play a major role in the thermal image of the plants under observation. The major aim of this project is therefore to combine analysis of stereo visual images with thermal images to overcome these problems and allow a precise 3-dimensional thermal profile of a crop to be quantified. This would then help the development of an integrated crop scanning system to identify significant temperature anomalies, hence providing growers with early warnings of possible crop disease or stress problems.

Summary

1. An experiment with impatiens where different irrigation treatments were applied (no watering, watering to 100% or 80% of previous days water loss) showed that thermal imaging could detect water stress in the unwatered treatment which had higher overall mean temperature. However, the images collected with the particular thermal camera used were not of good enough quality for detailed quantitative analysis. The figure below shows the resulting images from the experiment. The top row of plants which were watered to 100% previous day water loss appeared to be at the lowest temperature. The middle row of plants which were no watered appeared to be at highest temperature and the bottom row of plants which were watered to 80% previous

day water loss appeared to have temperature in between the temperature of top and middle row.

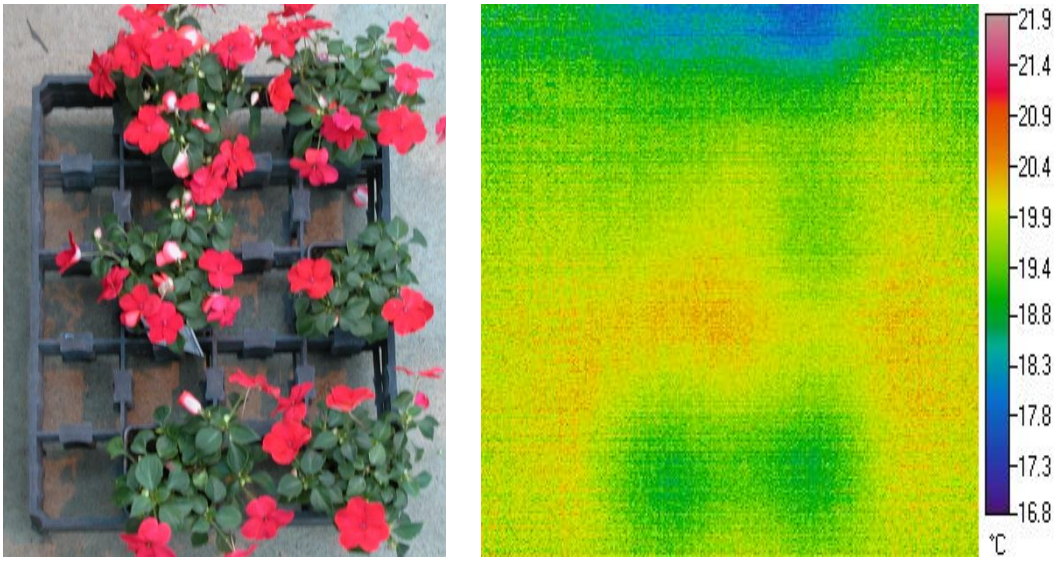

Figure 1: shows impatiens treated with different irrigation treatments. The top row was watered to 100% previous day water loss, the middle row was not watered and the bottom row was watered to 80% previous day water loss.

2. A new set up was developed to simultaneously capture stereo visual and thermal images of plants. Images of an *anthurium* plant were taken from the cameras at two different points horizontally displaced from each other. From the initial experiments it was observed that the plant regions which were higher from the ground appear to be at a higher temperature and the regions which were at an angle or further away from the camera appeared to be at a lower temperature. Quantitative analysis and modeling of the effect of height on plant temperature in the thermal image is currently underway which will help with the development of a rectified 3D thermal profile of a plant.

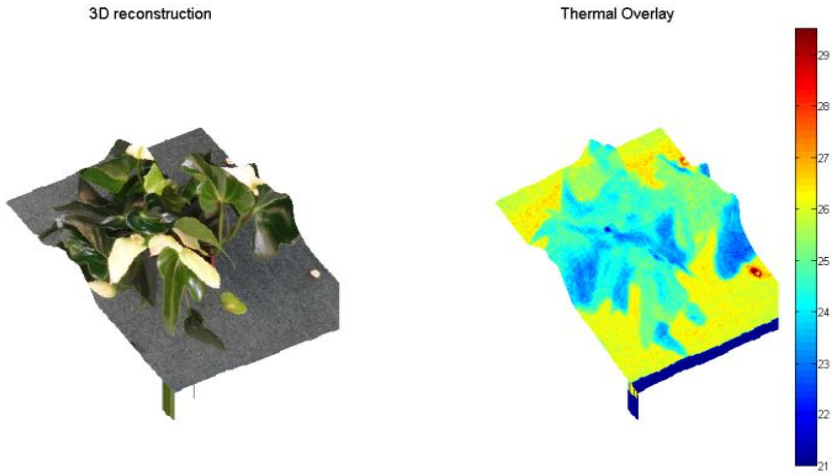

Figure 2: 3D reconstruction of plant and overlay of thermal image on the 3D reconstruction.

3. A new software application was developed and novel algorithms used to analyse high resolution thermal images of a spinach crop exposed to different irrigation regimes (image data provided by Ms. Hazel Smith and Prof. Gail Taylor at the University of Southampton). Water-stressed treatments had a higher average temperature, higher within image temperature variation and a distribution closer to a normal distribution compared to non-stressed treatments. The differences in distribution parameters were particularly useful in identifying water stressed plants. The figure below shows a snapshot of the software along with some initial results of the statistical analysis. The results show that the images with different type of treatments can be identified by statistically analysing the thermal images. The software is a work in progress and algorithm is being enhanced to find a better separation between thermal image of plants from different treatments.

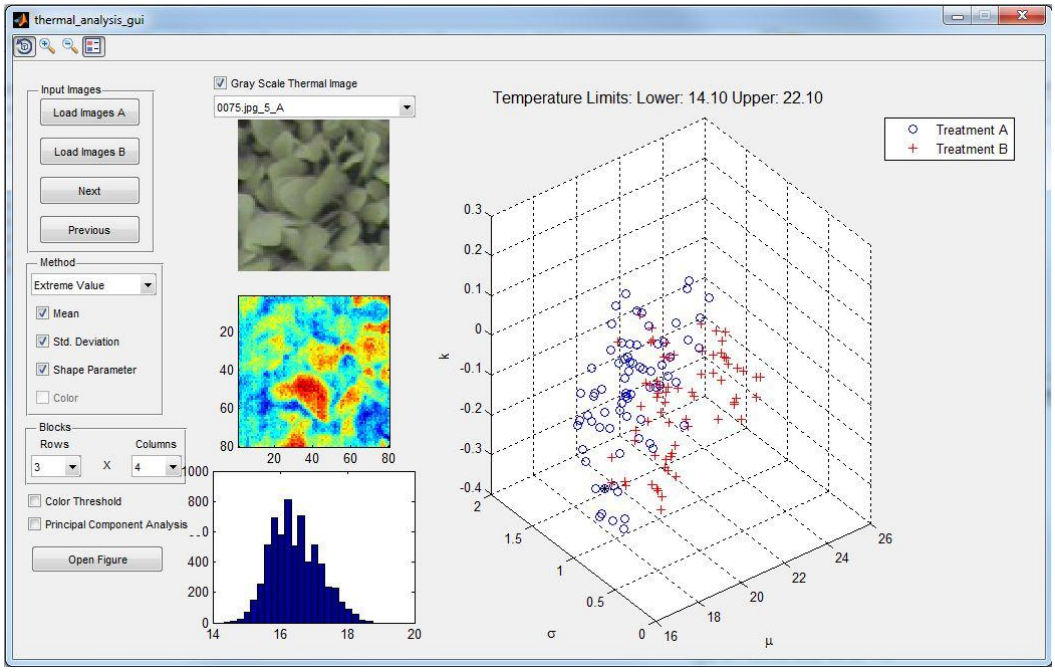

Figure 3: A snapshot of the software being developed to statistically analyse the thermal images of plants. The results show that the plants from different type of treatments can be separated by statistical analysis.

Financial Benefits

Financial assessment is premature at this stage, although it is anticipated that stress detection in different parts of the crop could help growers to water crops more efficiently and detect disease at an early stage facilitating timely action which would mitigate against crop losses and some of the costs associated with treatment.

Action point for growers

Glasshouse growers could consider options for installing an overhead system for monitoring their crop, pending further developments as this project progresses. The cost for a good thermal camera is around £15,000 – 20,000.

SCIENCE SECTION

Introduction

Thermal imaging was first developed for military purposes but now has been used for a wide range of applications in agriculture, industry, civil engineering, aerospace, medicine and veterinary. Thermal imaging converts the radiation pattern of an object to visible images. Similar to visual cameras, a thermal imaging camera comprises of a detector, signal processing unit and an image acquisition system. Since all objects above absolute zero temperature emit infrared radiations, for a thermal imaging camera infrared detector is used instead of a visible light detector.

There are two types of detectors used in thermal imaging cameras to detect IR radiation [1], thermal and photon detectors. In the thermal detectors, the infrared radiation heats the detector element which is taken as a measure of radiation falling on the detector. In photon detector, the radiation interacts at atomic or molecular level with the detector material, this interaction may involve interaction of photon and an electron, resulting electron to move through quantum energy levels and produce charge carriers that generate voltage across the detector. The photon detectors are more sensitive than thermal detectors, but they need to be cooled down for the electrons to come back to the desired energy levels for interaction. Thermal detectors do not require normally cooling, but they are less sensitive and provide lower resolution.

The non-contact and non-destructive nature and repeatability of measurements makes it quite useful in agriculture and food industry [2]. Leaf temperature in plants varies depending on internal and external factors. The environmental factors which effect leaf temperature via stomatal transpiration include solar radiation, air temperature, relative humidity and water status of the shoot. Thermal imaging has been used in predicting crop water stress, early disease detection in plants, determining genotype and phenotype, predicting fruit yield, bruise detection and detection of foreign bodies in food material. Thermal Cameras used by the researchers include FLIR systems Thermovision 900LW, Thermacam P25, Thermacam PM250, Thermacam SC2000, Varioscan 3201 ST, Infrared solutions Snapshot 225, IR Snapshot 525. Impac IVN 770-P is available at University of Warwick and was used in some experiments to collect some data.

In industry, *LemnaTec* has used infrared imaging combined with visible and fluorescent imaging for plant phenotyping [3]. They have developed hardware scanalyzer^{3D} which can take 3D visible images of the plants. It can scan the plants using different wavelength which include infrared, visible and fluorescent light. Infrared light helps to quantify temperature differences within leaves and plants. Plant health, nutrients, senescence and phenotype can

be studied using visible light images. Near infrared images are used to determine the water content of the soil. Scanalyzer ^{ESC} and Scanalyzer ^{HTS} have been developed to study phenotyping in environmental simulation chambers which take images of the plants using a moving camera or a conveyer. The latter is used for small plant phenotyping. Plant phenotype depends on the environment and its genome structure. Using the images, plant structures such as length, shape are used as features and can be tracked over time to determine plant phenotype under different environmental conditions.

Figure 1:Thermal imaging cameras Varioscan 3201(left), IVN 770-P (right)

Figure 2: ScanalyzerHTS developed by LemnaTec [3] to study plant phenotyping in simulated environments

In this report a brief review of the work in the field of horticulture with the help of thermal imaging is given. Section 2, 3 and 4 give a summary of the work done by various researchers with the help of thermal imaging for water stress, irrigation treatments, disease

detection, genotyping and phenotyping. Section 5 gives the summary of some existing literature on stereo vision in the field of horticulture. Section 6 give a summary of experiments conducted for image acquisition. Some of the preliminary results are discussed in section 7 of this part of the report.

Crop Water Stress Detection

Calculation of thermal Indices

Under water stress conditions, plants tend to close their stomata, and the transpiration rate is reduced. The reduced transpiration rate increases the leaf temperature which can be detected using the infrared thermometry or by the use of thermal imagers. Jones [4], [5] rearranged the leaf energy balance equation [6] and used the 'crop water stress index' (CWSI) [7], [8] to derive thermal indices, in equation (1),(2) and (3), based on 'wet' and 'dry' reference surfaces.

$$I_{CWSI} = \frac{(T_{leaf} - T_{wet})}{(T_{dry} - T_{wet})} \quad (1)$$

$$I_r = \frac{(T_{leaf} - T_{wet})}{(T_{dry} - T_{leaf})} \quad (2)$$

$$I_g = \frac{(T_{dry} - T_{leaf})}{(T_{leaf} - T_{wet})} \quad (3)$$

where T_{leaf} is the surface temperature of the leaf, T_{wet} and T_{dry} are the surface temperatures of wet and dry reference, I_{CWSI} is the index analogues to CWSI and I_r and I_g are the indices proportional to stomatal resistance and stomatal conductance. These new indices reduced the sensitivity of the method to environmental variations such as radiation, wind speed and air temperature. It was indicated that these reference surfaces must have a time constant close to those of real leaves to obtain better results.

Leinonen *et al.* [9] have studied and compared three main approaches for the estimation of stomatal conductance. The first approach uses the full energy balance equation [7] which calculates the stomatal resistance (inverse of stomatal conductance) by using only leaf temperature and environmental variables. The approach is prone to the highest probability of error because of its dependence on an accurate estimate of the amount of radiation absorbed by the leaf. The error can be reduced however, by taking measurements in a shaded canopy [10]. The second approach uses a modified energy balance equation [6] and uses only a dry reference surface. The analysis in the study shows that the use of dry reference is the most consistent and closest to porometer measurements. The third

approach uses both the dry and wet reference surfaces to decrease the requirement on the meteorological data [4]. The authors recommended using a dry reference instead of wet and dry, because it is difficult to maintain a reference leaf wet than to maintain it dry.

Grant *et al.* [11] have analyzed the robustness and sensitivity of thermal imaging for detecting changes in stomata conductance and leaf water status in plants. They found strong correlation between thermal indices [5] and stomatal conductance measured by porometry. Under water stressed conditions stomata close and leaf temperature rises. Conventional methods are time consuming whereas thermography was found to easily detect the temperature rise indicating drying soil. The authors compared precision of thermography and conventional water measurement methods in greenhouse conditions to provide an empirical assessment of the conditions in which thermal imaging can be reliably used against conventional methods. In a later study, Grant *et al.* [12] suggested that average temperature of the canopy was more useful to reduce the effect of leaf angles and other environmental factors than the individual leaf temperatures.

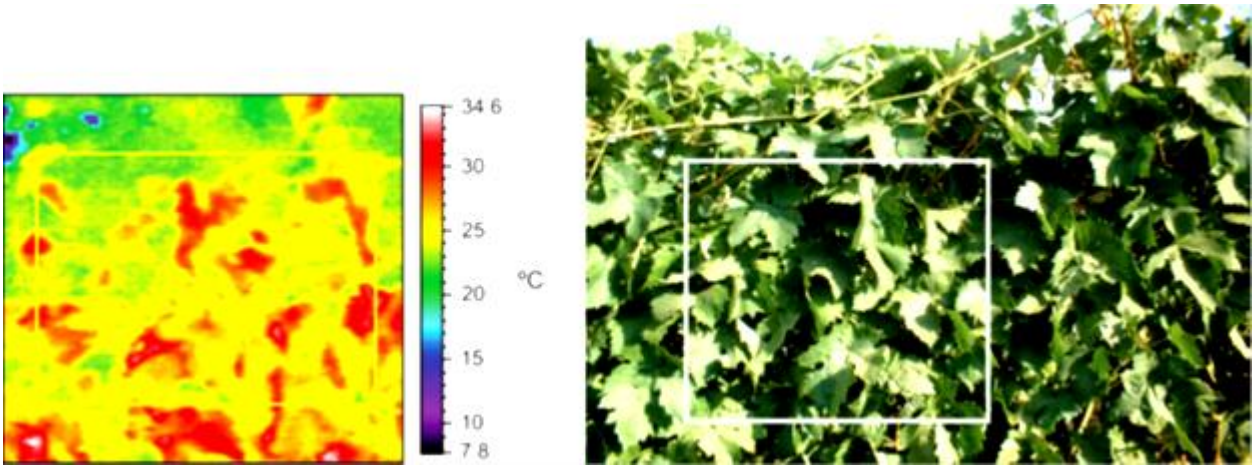

Figure 3: Thermal image and the corresponding visible light image is shown [12]. The area of interest is outlined to take the average of temperatures of leaves oriented at different angles.

The ambiguous assumptions in wetting leaves and inaccuracies in calculation of stomatal resistance were studied by Guilioni *et al.* [13]. According to the authors, the relationship between the leaf stomatal resistance, leaf temperature and temperature of two reference leaves varies according to type of leaf and the way in which the reference surfaces are wetted. The authors have given a table to clarify the ambiguities between these relationships, to select the relationship for different types of leaves, and to correct some erroneous expression in some earlier studies [4], [5], [9].

Temperature variation within canopies

Jones *et al.* [10] compared techniques for image acquisition and performed experiments to investigate the potential of infrared thermography for irrigation scheduling and to evaluate

the consistency and repeatability of measurements under a range of environmental conditions. Before the use of infrared imaging, infrared thermometers have been used for the thermal studies of the plants, infrared thermometers take an average over the target area and their measurements are likely to include non-transpiring tissues and extraneous surfaces (soil and sky) in their measurements. In an earlier study, Fuchs [14] concluded in his experiments that variance of leaf temperature (measured by infrared thermometer) gives a better estimate of leaf temperature than the average value. This limit does not apply to infrared imaging, since the temperature of the non-interested regions can be excluded from measurements. Jones *et al* [10], suggested to use wet and dry reference surfaces and to exclude any pixels which are outside the wet-dry threshold range to allow for semi-automated analysis of a large area of canopy. Temperature distribution between shaded and sunlit canopies was observed, sunlit canopies showed a wider range of temperature than the shaded canopies.

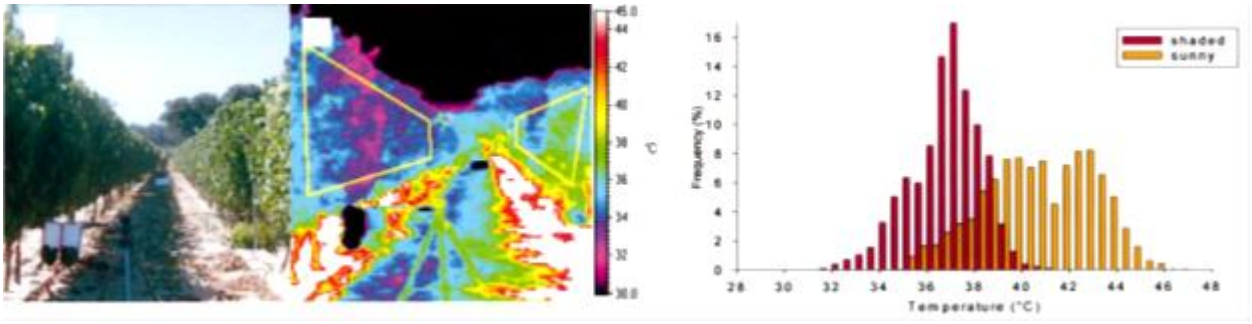

Figure 4: The shaded and sunlit sides (left) and the temperature frequency distributions for the outlined areas (right) [10].

However, the study of the variability was found to be dependent on scale of viewing, because large pixel size averages the leaf temperatures of different regions and therefore, an underestimate of true variability. Leaf temperature is more sensitive to stomatal conductance in sunlit leaves; it might seem that thermal data from sunlit leaves give a better estimation of stomatal conductance. However, the authors suggested using thermal data from shaded leaves with improved data consistency, since there is less variability in temperature within an image and smaller errors resulting from differences in radiation absorbed by reference and transpiring shaded leaves. They concluded from their experiments that canopy temperatures including the wet and dry references were dependent on crop water stress. Variation coefficients of stress indices [7] were found to be of considerable importance and discriminatory powers of the techniques for estimates of stomatal conductance were found to be limited. However, it was recommended that thermal imaging has great potential for comparative studies.

Visible imaging in stress detection

Möller *et al.* [15] studied the use of thermal and visible imaging to maintain mild to moderate water stress levels in grapevine. To estimate the canopy temperature different sections of the canopy were used in this study which includes all canopy, sunlit canopy, center of canopy, sunlit leaves from center of canopy. Best correlation between CWSI and leaf conductance was observed from the center of the canopy measurements (or its sunlit fraction). They observed a variation in slope between CWSI and stem water potential relationship with steeper slope observed in late summer. However, CWSI and leaf conductance relationship were found to be stable over time. This behavior shows an adjustment in plant response to higher leaf conductance during the summer while stem water potential remains the same. The authors studied the variance of canopy temperature and their relationship to crop water stress index as suggested by Fuchs [14]. They observed this relationship to be weak and statistically insignificant. They concluded from their experiments that Fuchs method might apply to homogeneous crops but not appropriate for row crops. They observed that CWSI computed with wet and dry reference was the most robust index and suggested that the fusion of thermal and visible imaging can not only improve the accuracy of remote CWSI determination but can also provide precise data on water status and stomatal conductance of grapevine.

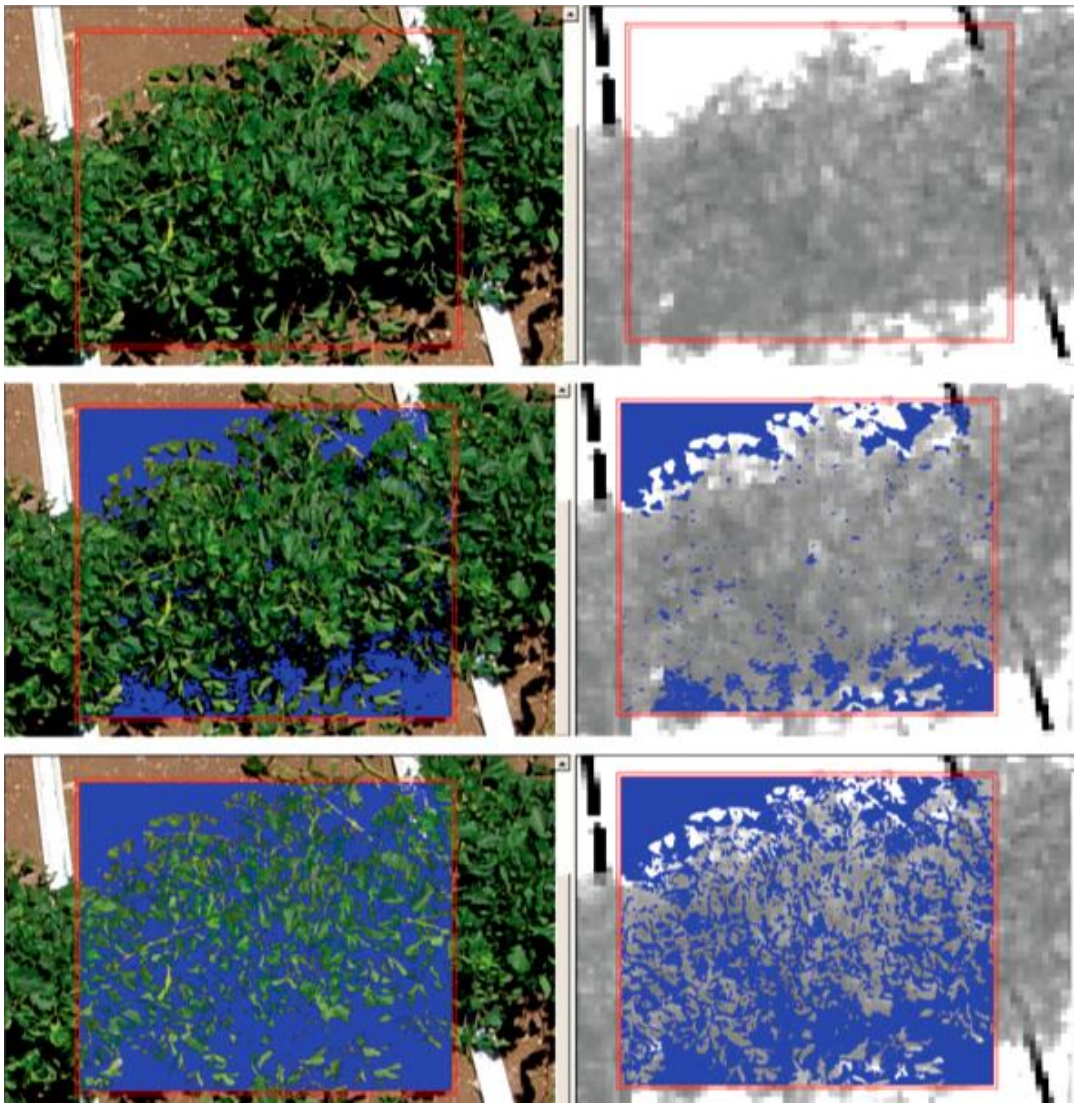

Figure 5: Use of thermal and visible images to extract different parts of canopy [15].

Leinonen & Jones [16] have used thermal imaging as a tool to identify plant stress. They combined thermal and visual images to identify leaf area and sunlit and shaded parts of the canopy. They used vaseline-covered and water-sprayed plants as dry and wet reference surfaces to reduce the effect of other environmental factors, which affect the canopy temperature, in calculations. They calculated the thermal indices [5] for single *Vicia faba* plants. These thermal indices were then compared with the stomatal conductance of the plants to quantify the relationship between temperature variation and stomatal conductance. As an initial preprocessing step, images of constant temperature background were subtracted from the actual image to correct for relative errors in calibration of camera caused by internal warming of camera. Ground Control Points (GCPs) were manually selected to overlay the thermal image on the visual image. Leaves in the visible images were manually identified as Regions of Interest (ROIs) for classification purpose to determine temperature distribution and to separate sunlit and shaded regions. The

temperature distribution can be used as an indicator of stomatal conductance and plant stress. Stoll and Jones [17] believed that the sunlit leaves show a wider range of temperature because natural leaf orientation has little effect on energy balance of shaded leaf, but large effect on exposed leaves. Based on these observations the leaf orientation temperature distribution varies in sunlit leaves and temperature distribution can be combined with the leaf orientation for thermal analysis in high resolution images.

Disease Detection

Thermal imaging has potential for early detection of disease, especially when the disease directly affects transpiration rate in plants, which is very important to control the spread of disease since late detection may result in reducing the quantity and quality of crop yield [18].

Salicylic Acid (SA) accumulation

Salicylic Acid (SA) is produced as a defense signal against pathogens in plants which induces metabolic heating and when applied exogenously to nonthermogenic plants increases leaf temperature. Chaerle *et al.* [19] studied the resistant tobacco plant infected with tobacco mosaic virus (TMV) and detected that the infected sites were 0.3-0.4°C warmer than the surrounding tissue 8 ± 1h before the initial appearance of the necrotic lesions. They used a localized-infection method and a high-resolution infrared camera to detect temperature increase at the site of inoculation. No measureable local or global change in leaf temperature was detected for near-isogenic but susceptible tobacco plants. They observed a correlation between leaf temperature and transpiration by thermography and steady-state porometry.

Study of cell death propagation

In a later study, Chaerle *et al.* [20] studied the propagating cell death in *bacterio-opsin* transgenic tobacco plants. They found that the cell death was trailed by coherent front of higher temperature. These spreading fronts were observed more in younger leaves, whereas isolated lesions were observed in older leaves. Cell death was first visible close to mid vein starting at the leaf base and subsequently, spread sideways and towards the leaf tip. Lower temperature was observed at regions with visible cell death because of water evaporation from the damaged cells. It was observed that the stomatal closure preceded the tissue collapse. They obtained high resolution thermographic images by capturing several slightly overlapping images and then registering them. The subimages were visualized within a temperature window of 1 °C, to maximize the temperature contrast.

Fluorescence imaging in disease detection

Chaerle *et al.* [21] have studied the use of thermal and chlorophyll fluorescence imaging in pre-symptomatic reponses for diagnosis of different diseases and to predict plant growth. Fluorescence imaging can be used at subcellular resolution but it is difficult to apply it to plant canopies outdoors. Thermal imaging can be applied to outdoor measurements at large scale but resolution is of the order of mm^2. However, both of these imaging methods can be applied for detecting and diagnosing plant stresses. Conventional weight loss and gas exchange measurement methods are time consuming and suitable for small number of plants whereas imaging techniques can be used to screen large number of plants for biotic, abiotic stress and to predict the crop growth.

Maximum Temperature Difference (MTD)

Oerke *et al.* [22] studied the changes in metabolic processes and transpiration rate within cucumber leaves caused by pathogenesis of *Pseudoperonospora cubensis*. Under controlled conditions, a linear relation was found between transpiration rate and leaf temperature. They showed that healthy and infected leaves can be discriminated even before the visible symptoms of the downy mildew (caused by *Pseudoperonospora cubensis*) appear. The maximum temperature difference (MTD) [23] was found to be related to the severity of infection and could be used for the discrimination of healthy leaves or canopies and those with downy mildew. Conditions enhancing transpiration rate improved the detection of these changes at an early stage of infection.

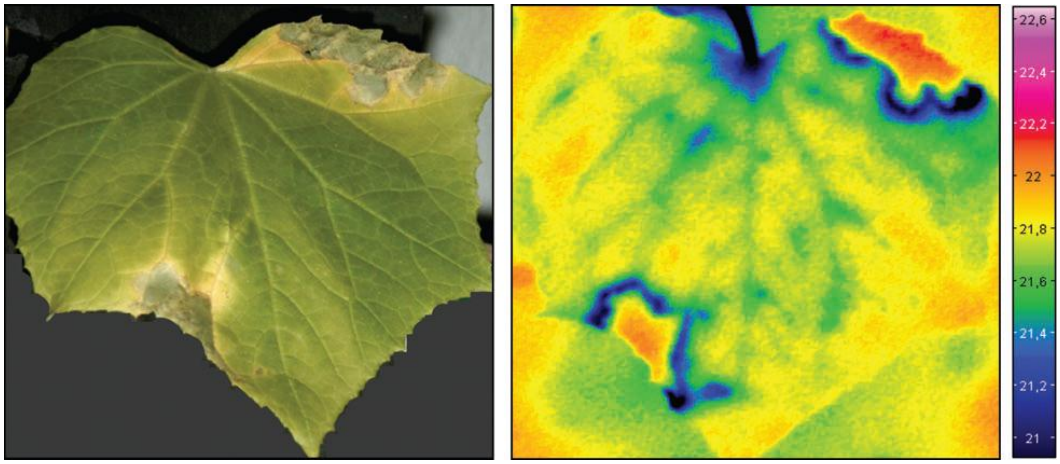

Figure 6: Symptoms of downy mildew appear as zones of different temperatures on cucumber leaves 7 days after inoculation with *Pseudoperonospora cubensis* [22].

Analysis of diseased plants with different irrigation treatments

Stoll *et al.* [24] have investigated the use of infrared thermography to study the attack of *Plasmopara viticola* in grape vine leaves under varying water status conditions. They applied and studied different irrigation treatments for both inoculated and non-inoculated

vines. They observed that there were statistically significant differences between slopes of regression when comparing inoculated and non-inoculated treatments, whereas no statistically significant difference were observed when irrigated and non-irrigated treatments were compared.

Phenotyping

Jones *et al.* [25] explored the potential of thermal imaging for crop phenotyping and irrigation management purposes from single leaves in controlled environments to canopies in large fields. The authors studied the variation of leaf and canopy temperature as a function of radiant energy absorbed by the leaves. They studied the reflectance effect on the leaves as the view angles changes relative to incident solar light and how it affects the average leaf temperature observed by the imaging equipment. Temperature differences between areas of canopy corresponding to different irrigation treatments and phenotypes were studied. Temperature difference succeeded in identifying individual plots with different genotypes.

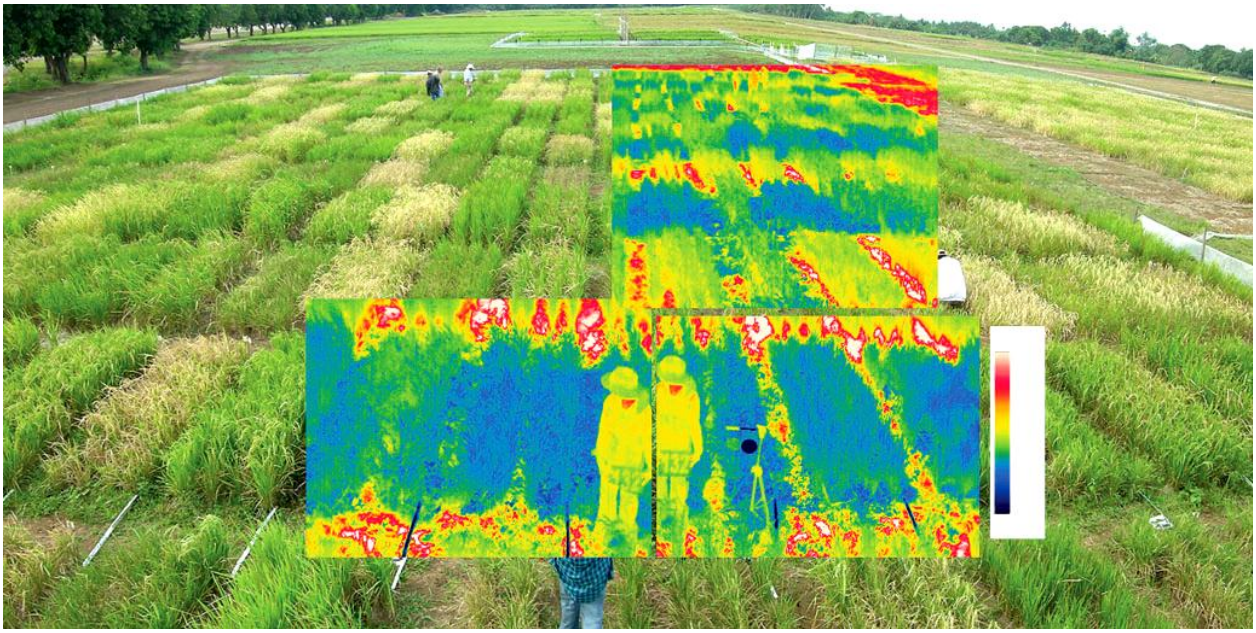

Figure 7: Visible light image, with corresponding thermal images, of a rice 'macro array' trial in the dry season of 2006 consisting of 300 plots combining 50 contrasting genotypes, two water treatments (well watered and drought stressed) and three replicates at the International Rice Research Institute [25].

Merolet *et al.* [26] investigated the effectiveness of thermal imaging for high through-put screening of *Arabidopsis* mutants defective in stomatal regulation. Altered stomatal control affects transpiration which can be detected as a change in leaf temperature. Plants synthesize Abscisic acid (ABA) hormone to trigger closure of stomatal pores. The authors observed that the leaf temperature of wild type plants was high after 3 days of drought stress, whereas ABA-insensitive and ABA-deficient mutants failed to close their stomata

and were colder. The amount of ABA present in the leaves was quantified to identify for ABA-insensitive mutants and ABA-deficient mutants.

Stereoscopy

The effect of leaf angles and the distance of the plant from the thermal image sensor has been studied by various researchers [25], [12]. Grant *et al*. [12] suggested to take average temperature of the canopy to reduce the effect of leaf angles. However, there is very little literature on the quantitative analysis of effect of angles of an object on its thermal profile [27]. Stereoscopy is a technique which can be used to estimate 3D depth of points in a scene by finding matching pixels corresponding to these points from two or more 2-dimensional images. The simplest setup used for stereovision is the parallel camera setup which uses two identical cameras on a horizontal plane with parallel vertical and optical axis as shown in Figure 8. For this setup, correspondence between the points in the images is in the form of relative displacements or disparities. The following section in the report discusses some of the existing literature to estimate disparity in stereo vision.

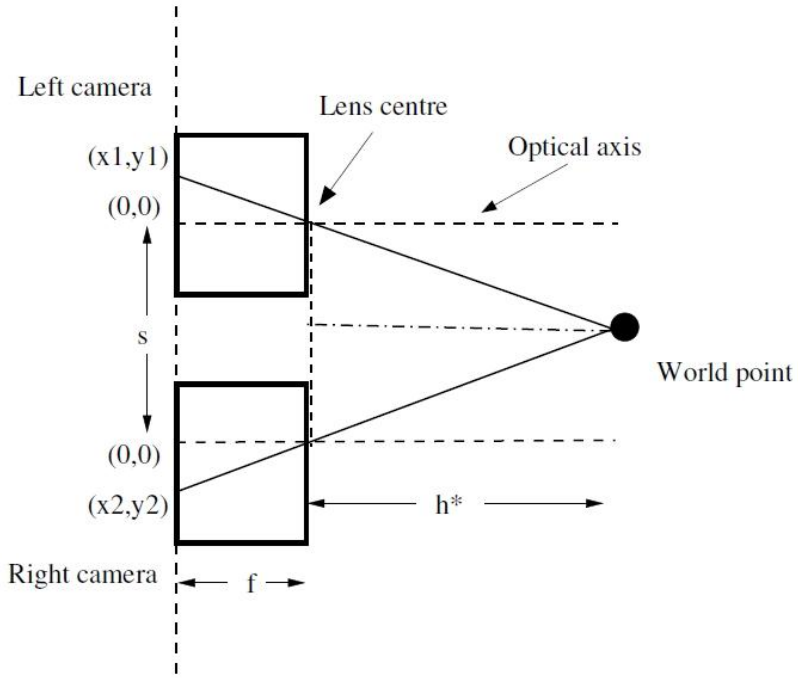

Figure 8: Parallel camera setup Model [28]. (*x*1, *y*1) and (*x*2, *y*2) are the pixel locations on which the world point is projected. s is the seperation distance between the cameras. h* is the distance of the object point from the camera [28].

Disparity Estimation for Stereo Vision

Most stereo vision algorithms compute disparity with respect to a reference image which could be one of the input images. The main challenges involved in the disparity estimation include noise, textureless areas, depth discontinuities, non-Lambertian surfaces and

occlusions. A lot of work has been done by researchers [29] to meet these challenges and different techniques have been proposed which can be categorized into feature based, window based and energy based approaches [30]. Feature based approaches are fast and give accurate estimation of the measure of correspondence between the points in images, however they suffer a major drawback that they produce sparse disparity results. Window based approaches use intensity values within a finite window and can have very efficient implementations that are suitable for real time applications. However, these methods assume constant disparities within a window, which is incorrect at discontinuities and leads to blurred object boundaries. Energy based approach make explicit smoothness assumptions and solves energy optimization problems. These approaches produce dense disparity maps however they are computationally and memory intensive.

Fua [31] has presented an approach based on correlation to compute dense depth maps and preserve depth discontinuities in real world scenes. The author has designed the algorithm to perform a consistency check to reject invalid matches. The validity criterion proposed by the author is based on a right/left match in which the two images play a symmetric role and that allows to reliably use small windows. The algorithm performs the correlation twice by reversing the role of the two images and consider as valid only those matches for which depth measured is same for corresponding points. A hierarchical approach has been used i.e., use windows of a fixed size to perform the matching at several levels of resolution. To introduce depth discontinuities, the method uses interpolation technique by combining the depth map and the grey level information in the image.

Birchfield & Tomasi [32] have introduced a measure of dissimilarity which according to the authors is insensitive to sampling. To compute dissimilarity between the pixels the method uses the linearly interpolated neighbouring intensity pixels and the absolute difference. The authors have shown that the dissimilarity measure works as long as there is no high frequency signal present in the intensity function. But they have shown with experiments that it still works better than absolute difference for high frequencies.

Konolige [33] has discussed the implementation of the area correlation-based stereo algorithms for real-time applications. Area correlation methods usually attempt to compensate by correlating not the raw intensity images, but some transform of the intensities e.g., Normalized intensities, Laplacian of Gaussian or nonparametric transformation. The author suggests that the best quality results appear to come from absolute difference of the LoG, and from census [34]. The suggested algorithm comprises of the following steps:

1. Prefiltering using LoG transform to normalize image brightness and enhance texture.
2. Correspondence search along horizontal epipolar lines using a SAD window.

3. Postfiltering with an interest operator and left/right check to eliminate bad matches.

Since, textureless regions give less reliable measure of disparity than the textured regions, the last step uses measure of texture in a scene as an interest operator which gives high confidence to areas that are textured in intensity.

Scharstein and Szeliski [29] have built a standard dataset with ground truth disparity estimate and have classified and evaluated different correspondence algorithms on this dataset. According to the analysis done by the authors, stereo correspondence algorithms generally perform four steps which include cost computation, cost aggregation, disparity estimation and disparity refinement. The common matching costs include squared differences, absolute differences, mean square error, mean absolute difference. Local and window-based approaches aggregate the matching cost by summing, averaging or by using weighted values of neighboring pixels within a support region defined by the algorithm. Final estimated disparity is then the disparity associated with the minimum cost value. Some algorithms apply a sub-pixel refinement step using splines and other interpolation techniques.

Klaus *et al*. [35] have presented a segment-based stereo matching approach. The algorithm utilizes colour segmentation on the reference image and instead of assigning a disparity value to each pixel, a disparity plane is assigned to each segment. Segment-based methods generally perform four consecutive steps. First, regions of homogeneous colour are located by applying a colour segmentation method. Second, a local window-based matching method is used to determine disparities of reliable points. Third, a plane fitting technique is applied to obtain disparity planes that are considered as a label set. Fourth, an optimal disparity plane assignment (optimal labelling) is approximated using greedy or graph cuts optimization. Mean-shift colour segmentation has been used by the authors because it has the advantage that edge information is also incorporated. The approach uses a weighed combination of absolute intensity differences and a gradient based measure. An optimal weighting ω between absolute differences and gradient measure is determined by maximizing the number of reliable correspondences by applying a left/right in conjunction with a winner-take-all optimization (choosing the disparity with the lowest matching cost). A matching cost is calculated in a segment to plane assignment and disparity plane with minimum matching cost is assigned to each segment.

Kim *et al*. [36] have approximated mutual information to a standard energy minimization problem. Comparing fixed-size windows via mutual information suffers from poor performance at discontinuities and in low-texture regions. The key advantage of mutual information is its ability to easily handle complex relationships between the intensities in the two images. The authors have exploited this advantage of mutual information by converting mutual information to an energy minimization problem using Taylor series approximation.

The energy can then be efficiently minimized using graph cuts, which preserve discontinuities and handle low-texture regions. The resulting algorithm combines the accurate disparity maps that come from graph cuts with the tolerance for intensity changes that comes from mutual information.

Hirschmüller [37] has introduced a semi global matching based on the work done by Kim *et al*. [36]. The method uses a hierarchical approach to perform pixelwise matching of Mutual Information and approximates a global smoothness function. The first step is the hierarchical pixelwise disparity estimation to obtain a disparity image. The second step adds a smoothness constraint which penalizes for the changes in neighbouring disparities in the disparity image. For small changes, small constant penalty is added whereas for large changes large constant penalty is added. This allows adaptation to curved surfaces as well as to discontinuities. The author has extended his work in [38] for disparity refinement and for processing huge images. The refinement step removes small patches of disparity which appear as peaks, which leads to holes in the disparity image. In this work, invalid disparities have been classified into occlusions and mismatches using left/right consistency check. Occlusions have not been interpolated but mismatches have been interpolated from neighbouring pixels to produce dense disparity map. Image segmentation using Mean Shift Segmentation algorithm and plane fitting has been used for refining initial disparity image. To process huge images a solution is proposed to divide the image into tiles and compute the disparity of each tile individually. The method has been evaluated with Middlebury stereo dataset and has been shown to perform superior to other methods.

In another work Hirschmüller & Scharstein [39] have evaluated the insensitivity of different matching cost functions to radiometric variations. Radiometric differences can be caused by cameras due to different settings e.g., vignetting, image noise or reflection due to non-Lambertian surfaces. The authors produced image sets with artificial radiometric variations and evaluated different cost functions using three stereo algorithms, window based, semi-global and Graph cuts methods. The authors concluded that the performance of a matching cost function depends on the stereo method that uses it. Rank filter appears to be the best matching cost for correlation based methods. Hierarchical Mutual Information (HMI) [37] appears to be best for pixel-based matching methods like Semi-Global Matching and Graph Cuts in the presence of global brightness changes and noise. In the case of local brightness variations such as vignetting; Rank and LoG appear to be better alternatives than HMI. However, none of the matching costs compared in this study were very successful at handling strong local radiometric changes caused by changing the location of the light sources. The authors extended the work in [40] and have included more cost functions to their evaluation study. The results on images without radiometric changes show that Bilateral filtering with background subtraction and Census filtering produce best results with

three stereo methods. HMI works equally well for global and semi global method on some data sets. When tested with images with simulated radiometric changes, Census appears to be more robust and best in many cases. HMI is more stable to image noise but it performs worst on images with local changes like strong vignetting. Census performed very well throughout all experiments with simulated and real radiometric differences, except in the presence of strong image noise. HMI compensates for complex global radiometric relations between the input images. It performed slightly better than Census in case of low radiometric changes and pixelwise matching using the semiglobal or global stereo method. It also performed best in case of strong image noise. However, HMI showed problems with large local radiometric differences, caused, for example, by the vignetting effect and by non-Lambertian surfaces and lighting changes.

Song *et al*. [28], [41] have introduced a multi-resolution approach for surface modelling of plants. The author has used matching cost function introduced by Birchfield & Tomasi [32] for each colour channel to compute disparity. A Gaussian pyramid scheme has been used to speed up matching each level represented as nodes. To prevent the propagation of poor results from false matches to parent nodes, a weighing method is applied which takes weighed input from the neighbouring parent nodes. Kalman update is applied to the nodes at each level and the disparities estimated are converted into depths by triangulation.

Stereoscopy in Plant Imaging

Stereo vision can be used to automate quality estimation of plants such as pansy and poinsettia which are characterized by a number of attributes. Song *et al*. [41] have used stereo vision to model the important characteristics of plants. The authors used a multi-resolution strategy as discussed above for disparity estimation and self-organizing maps to model the plant surface. The model can be used to extract useful plant features which can be used for industry application such as crop scheduling and plant growth management.

Parsons *et al*. [42] have used the technique [41] for quality assessment of ornamental crops in glasshouses. The manual measurement and visual inspection of which is highly labor-intensive. The authors have used the colour information and Artificial Neural Networks to obtain quality scores for dianthus, viola and cyclamen. They have compared quality scores obtained from image analysis with the quality scores obtained from a panel of assessors. They found that the image analysis quality scores were more reliable than the panel scores. The authors further stated that these image analysis methods can be combined with the additional sensors to detect localized pests and disease.

In a latter work, Song *et al*. [43] presented an approach to combine stereo vision with Time-of-Flight (ToF) images to estimate depth maps for plant phenotyping. Time-of-Flight cameras use speed of light to generate a coarse resolution image representing the distance

of an object. The authors have shown that stereo vision when combined with ToF images give a better estimate of the depth map and can be used to automatically estimate phenotypic characteristics such as leaf area stem length or fruit size.

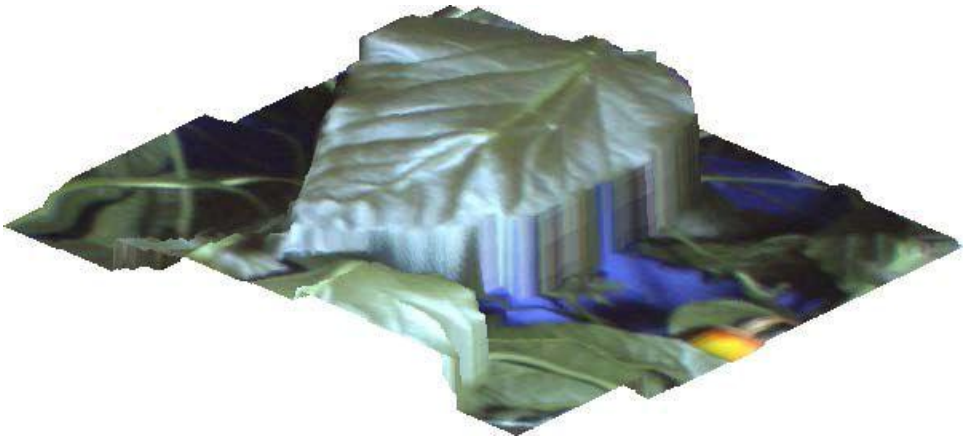

Figure 9: Surface reconstruction for Leaf using depth estimates by combining stereo and ToF results [43]

Materials and methods

Image Acquisition Experiments

An experiment was setup to collect thermal images at the Wellsbourne campus at University of Warwick with the help of Dr. Andrew Thompson. Figure 10 shows the experimental setup used to collect the images of impatiens with different irrigation treatments.

Figure 10: Experimental Setup to collect images of impatiens with different irrigation treatments

In this experiment, three types of irrigation treatments were applied to impatiens. In treatment 1, plants were watered equal to the amount of water they lost previous day, in treatment 2 plants were watered equal to 80% of water lost previous day, and treatment 3 plants were not watered at all. After 5 days of different irrigation treatments temperature differences appeared in the thermal images. Plants treated with different treatments were observed to be at different temperatures as shown in Figure 11. In the top row in Figure 11 are the plants which were watered to their field capacity every day and they show a lower temperature, the plants in the bottom row were treated with treatment2 and show higher temperature than the top row, the plants in the middle row were treated with treatment 3 and show the highest degree of temperature in the whole image. However, the images collected by the help of the thermal camera were not of very good quality.

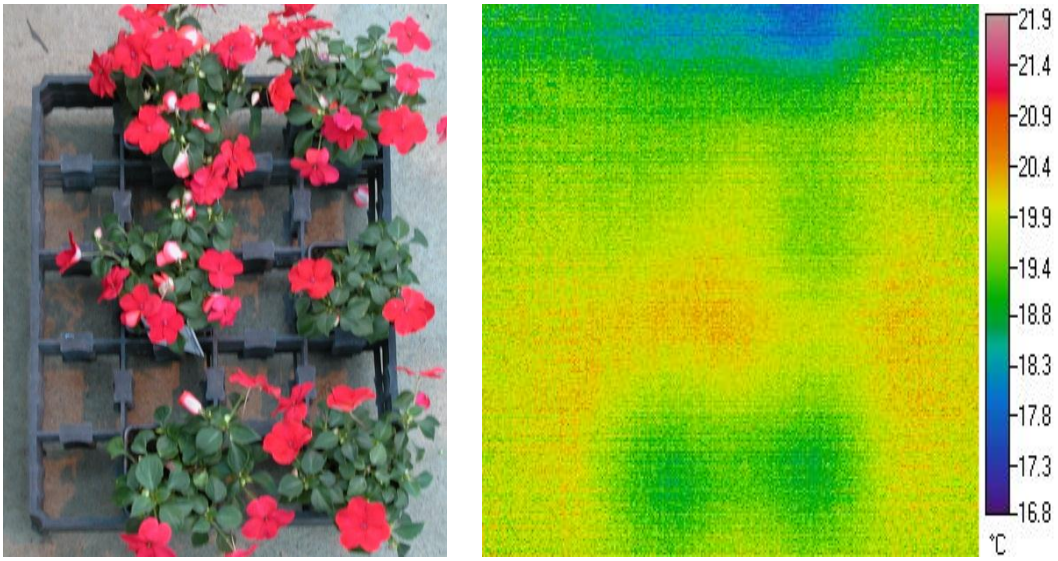

Figure 11: shows impatiens treated with different irrigation treatments. The top row was treated with treatment 1, the middle row with treatment 3 and the bottom row with treatment 2.

A setup is being developed at Computer Science Department to simultaneously capture stereo visual and thermal images of the plants. A camera can be mounted on a movable platform which can be used to take two (or more) pictures of a scene from horizontally displaced positions. A picture of the setup is shown in Figure 12. The setup is in development phase and experiments are being carried out to make accurate measurements of the depth from the images. In our experiment, we horizontally displace the camera in small steps and take images of different plants (or test objects) at each step. Manual measurement of the height is taken and the algorithm is tested to estimate the actual height. Results of the disparity estimate along with a thermal overlay are shown in preliminary results.

Some good quality thermal and visual images were also collected by our collaborators Hazel Smith and Gail Taylor at the University of Southampton and these images were used for further analysis.

Figure 12: Setup to capture stereo and thermal Image

Preliminary Results

Stereo Setup

Images of an *anthurium* plant were taken from a camera at two different points horizontally displaced from each other. The images taken from left and right camera position are shown in cyan and red color in Figure 13. A disparity map overlaid on the plant image is shown in Figure 14. Figure 15 shows disparity overlaid on plant image and on thermal image. It has been observed that the regions of the plant which are higher from the ground and thus have more disparity, show higher temperature whereas plant regions which are at a lower height or at an angle show lower temperature. The quantitative analysis of the height variation to plant temperature is in progress.

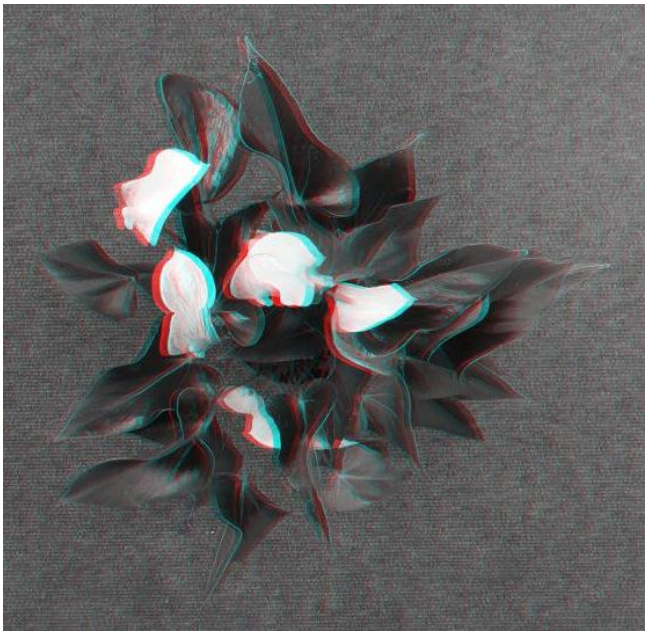

Figure 13: Images of the same plant captured from two different positions. Image taken from right is shown in red and image taken from left is shown in cyan color.

Figure 14: Overlay of disparity on plant image

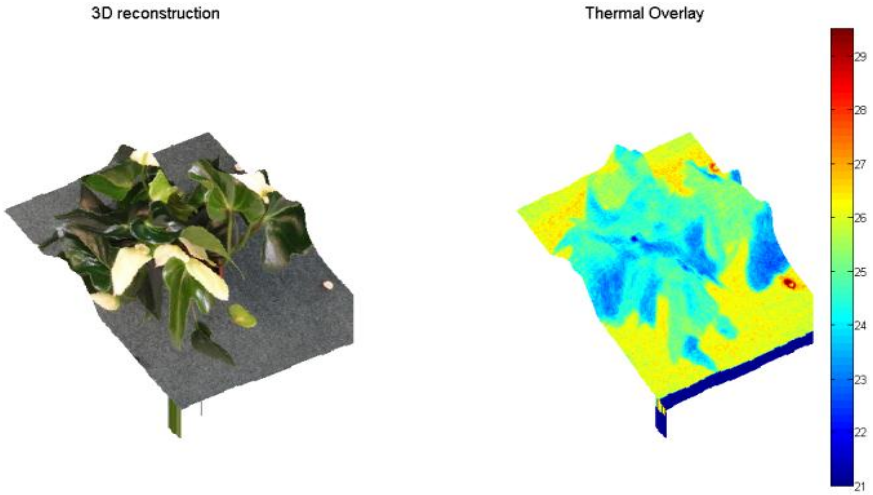

Figure 15: 3D reconstruction of a plant image and overlay of thermal image on dispartity.

Drought Experiment

Images of a spinach canopy from a drought experiment were obtained from the collaborators at University of Southampton. The images from well-watered canopy were termed as treatment A and the images from plants under water stress were called treatment B images. Some of the images of crop with two different treatments along with their histogram are shown in Figure 16 and Figure 17 below. In the images of crop with treatment A lower average temperature, less temperature variation within image and more skewed distribution was observed as shown in Figure 16. In the images with treatment B, higher average temperature, higher within image temperature variation and distribution close to normal distribution was observed as shown in Figure 17. Based on these observations some experiments were carried out on the images belonging to both the treatments.

In one of the experiments, all the thermal images were divided into twelve sub-images (3 rows and 4 columns) and the mean of the intensity values was calculated for each sub-image. Standard Deviation among the mean values was calculated and plotted against mean of intensity values of the whole image; the result is shown in Figure 18.

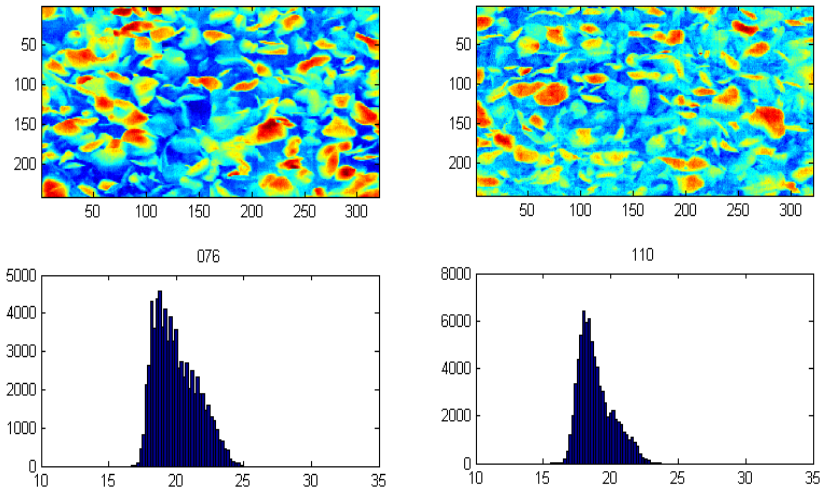

Figure 16: shows crop images with treatment A, more uniform temperature distribution was observed in the image and the histogram of the images with this type of treatment were observed to be skewed.

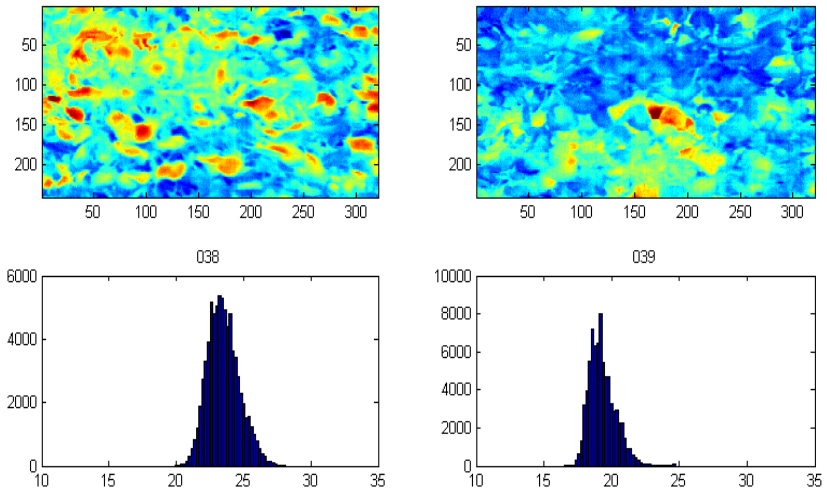

Figure 17: shows crop images with treatment B, discrete zones with different temperature were observed in the image and the distribution was close to a normal distribution.

In Figure 18, the blue circles show the points from images belonging to treatment A, and the red circles show the points belonging to images from treatment B. From the plot it was observed that images from both treatments can be separated on the basis of the standard deviation among the mean values of the sub-images.

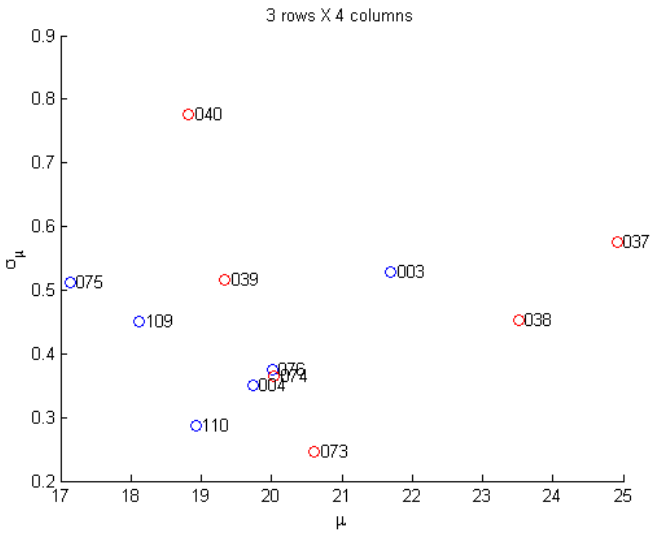

Figure 18: The plot shows mean of intensity values of whole image on x-axis and standard deviation among mean values of blocks on y-axis.

The distribution was also compared with generalized extreme value distribution and maximum likelihood estimates of the parameters for mean, standard deviation and shape parameter for the distribution were obtained. The results obtained were plotted on a 3D plot

as shown in Figure 19. The plot shows that the images from the two treatments can be separated on the basis of parameter estimates of the distribution.

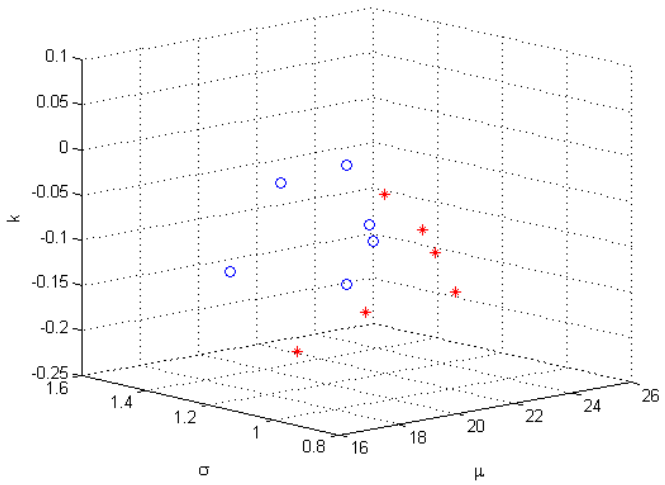

Figure 19: Parameter estimates of the distribution of the images with different treatments. Blue circles belong to treatment A and red asterisk belong to data of images from treatment B.

Since, the data was limited for the above experiment, more data was artificially generated by dividing each image into 12 sub-images (generating 144 images, 72 for each treatment) for analysis. The parameter estimates are plotted in Figure 20 which show that the images from different treatments can be separated on the basis of these parameter estimates of distribution.

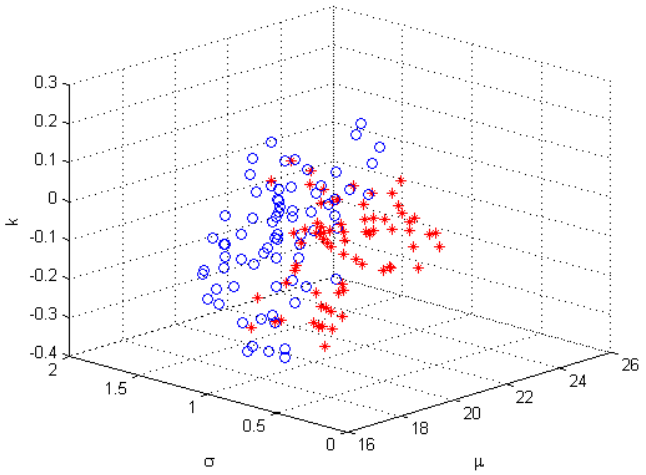

Figure 20: Parameter estimates of the distribution for artificially generated large dataset of images. Blue circles belong to treatment A and red asterisk belong to treatment B.

Software

Software with a graphical user interface has been developed to statistically analyze spinach data. A snapshot of the software is shown in Figure 21.

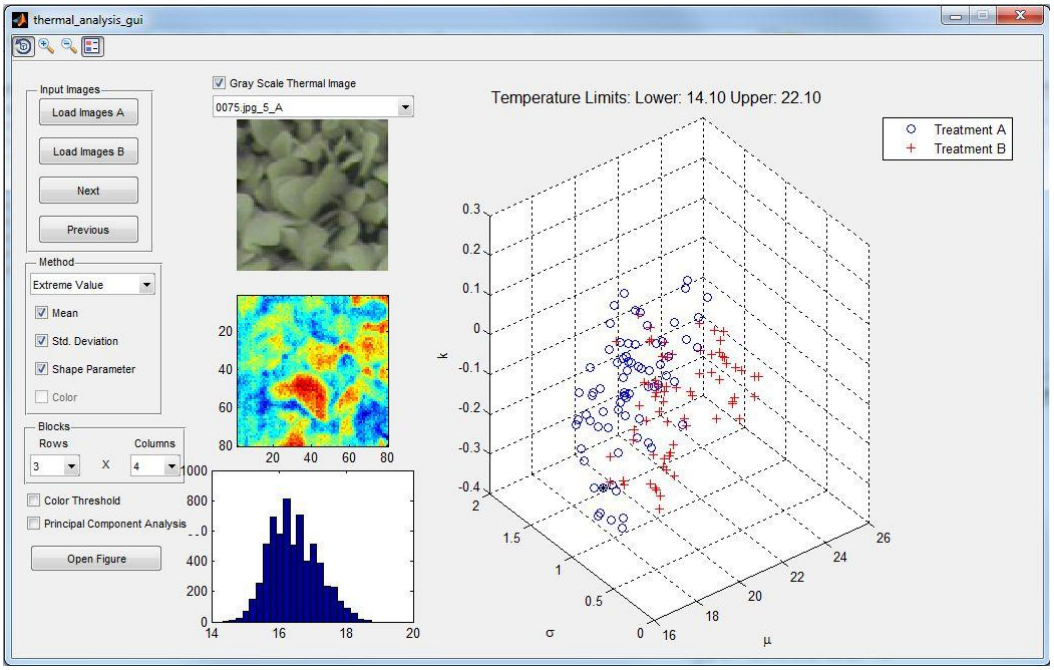

Figure 21

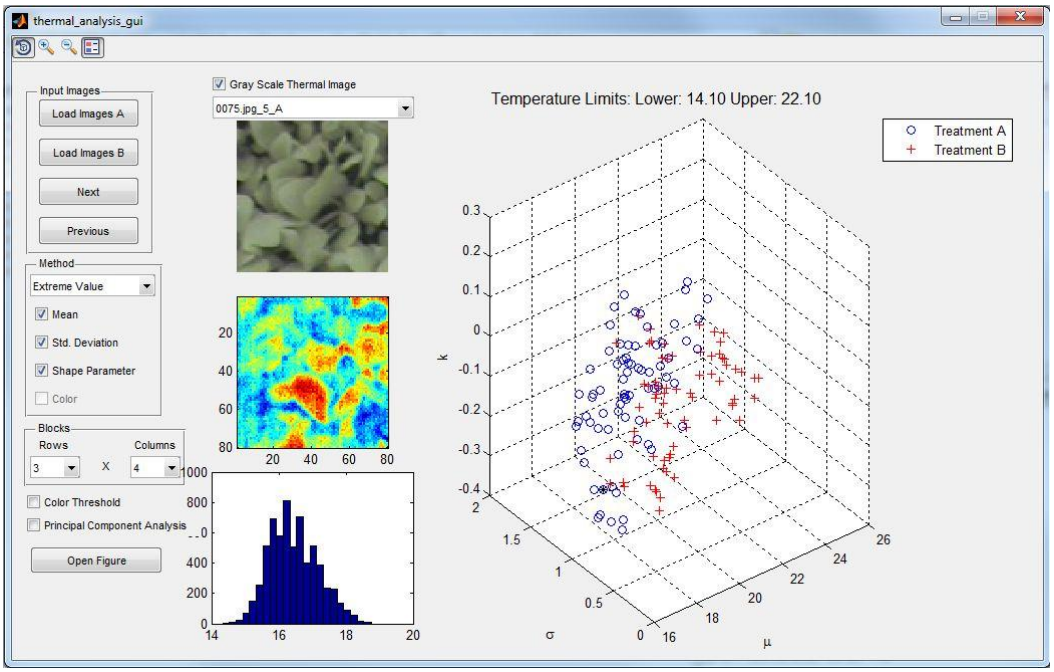

Figure 21: Snapshot of the Software for analysis, watch video at http://youtu.be/aubBgRDPOaM

The software takes images from treatment A and treatment B as input. Treatment A and B images are not restricted to this drought experiment and can be from any experiment with two different types of treatments. The software plots a scatter plot of the statistical

parameters of the thermal images. The user can select the statistical parameters of interest. If the user is interested in any point on the plot, the user can view the image corresponding to that point by clicking the point in the plot, making analysis easier. The software can be used to divide the image into a grid of sub images, to make analysis on specific part of image. The software can also be used to apply color threshold and can use Principal Component Analysis to generate uncorrelated data.
A video presentation of the software operation can also be viewed at the link below[1].

Liaison with the commercial growers

To better understand industry requirement and the challenges they face it is important to interact with them. Following visits were made to the following Nurseries/Conferences during the year 2011/2012.

Date	Place	Purpose
7 Jul 2011	BordonHill Nursery	Discussed options with the nursery to install stereo and thermal imaging setup
9 Nov 2011	Roundstone Nurseries	Attended BPOA Poinsettia meeting and Grosouth trade exhibition
17 Jan 2012	Warwick Crop Center	Presented the potential of thermal imaging for the benefit of growers and some initial results.
06 Feb 2012	Hellidon Lakes Hotel Leicester	Attended BPOA AGM and Technical Seminar

Conclusions and Future Work

Our preliminary results on thermal data with water stress experiments suggest that thermal imaging can be a useful tool to remotely detect and monitor physiological changes in plants. In the literature review section, it has been observed that leaf angles, sunlit and shaded regions and environmental conditions can also play a major role in the thermal image of the plants under observation. There is currently disagreement among researchers on whether to use thermal data from shaded or sunlit regions of the canopy because in shaded regions thermal data has been found to be more consistent whereas in sunlit regions more variability has been found in the data. There is also some disagreement on using average or variation in the thermal data as a measure of crop water stress. It would be useful to investigate on these issues on which the researchers disagree.
In particular, the following issues will be addressed in the next 6-12 months:

[1] http://youtu.be/aubBgRDPOaM

1. The line of action would be to collect more good quality thermal and visual image data, create a depth map of the plant/object under observation, and then overlay the thermal data on the 3D model. From the depth map, the leaf angles can be calculated and the intensity of pixels in the thermal image can be recalibrated for further investigation since the intensity of pixels in the thermal image depends on the leaf angles.
2. For acquisition of good quality images, the camera needs to be fixed on a frame to collect data from plants under same conditions. The existing thermal camera does not have a high thermal and spatial resolution and it has a very limited field of view which means the camera has to be mounted high above the plant to collect good quality thermal of the whole plant surface. An application for an internal Research Development Fund (RDF) award to buy a new thermal image camera was been made in May. The proposed thermal camera FLIR P620 will have higher spatial and thermal resolution i.e., 0.65mrad and 640x480. The integrated (3.2 MP) visual camera will help to make the analysis fast and more accurate.
3. In our experiments with the Southampton data, the images were divided into several sub-images to create a dataset for analysis. For further analysis, more good quality data and deeper analysis of the temperature distribution is required. We are working in close collaboration with the University of Southampton to get hold of their reasonably good quality data for the water stress experiments. We envisage that our model and the algorithms developed for various different water stress treatments will be directly applicable to disease versus normal, since a diseased plant will show signs of increased temperature distribution similar to a plant undergoing water stress. An experiment for validating our model and algorithms for disease detection and monitoring is being set up at the Warwick Crop Centre with the help of Dr John Clarkson to collect some more data for powdery mildew in tomato.
4. A visit to Double H nurseries has been made during the HDC conference in July and options to install a thermal and stereo imaging setup have been discussed. Whole canopy images will be collected after the camera setup is installed at the nursery.

References

[1] T. L. Williams, “Thermal imaging cameras and their component parts,” in *Thermal Imaging Cameras: Characteristics and Performance*, CRC Press, 2009, pp. 7-33.

[2] R. Vadivambal and D. S. Jayas, “Applications of thermal imaging in agriculture and food industry—A review,” *Food and Bioprocess Technology*, vol. 4, no. 2, pp. 186-199, Feb. 2010.

[3] M. Eberius, “Automated image based plant phenotyping - Challenges and chances,” *2nd International Plant Phenotyping Symposium*, Jülich, 2011.

[4] H. G. Jones, “Use of infrared thermometry for estimation of stomatal conductance as a possible aid to irrigation scheduling,” *Agricultural and Forest Meteorology*, vol. 95, no. 3, pp. 139-149, Jun. 1999.

[5] H. G. Jones, “Use of thermography for quantitative studies of spatial and temporal variation of stomatal conductance over leaf surfaces,” *Plant, Cell and Environment*, vol. 22, no. 9, pp. 1043-1055, Sep. 1999.

[6] H. G. Jones, *Plants and Microclimate*, 2nd ed. Cambridge: Cambridge University Press, 1992, p. 428.

[7] R. D. Jackson, S. B. Idso, R. J. Reginato, and P. J. Pinter, “Canopy Temperature as a Crop Water-Stress Indicator,” *Water Resources Research*, vol. 17, no. 4, pp. 1133-1138, 1981.

[8] S. B. Idso, R. D. Jackson, P. J. Pinter Jr, R. J. Reginato, and J. L. Hatfield, “Normalizing the stress-degree-day parameter for environmental variability,” *Agricultural Meteorology*, vol. 24, no. 1, pp. 45-55, 1981.

[9] I. Leinonen, O. M. Grant, C. P. P. Tagliavia, M. M. Chaves, and H. G. Jones, “Estimating stomatal conductance with thermal imagery,” *Plant, Cell and Environment*, vol. 29, no. 8, pp. 1508-1518, Aug. 2006.

[10] H. G. Jones, M. Stoll, T. Santos, C. de Sousa, M. M. Chaves, and O. M. Grant, “Use of infrared thermography for monitoring stomatal closure in the field: application to grapevine,” *Journal of Experimental Botany*, vol. 53, no. 378, pp. 2249-2260, Nov. 2002.

[11] O. M. Grant, M. M. Chaves, and H. G. Jones, “Optimizing thermal imaging as a technique for detecting stomatal closure induced by drought stress under greenhouse conditions,” *Physiologia Plantarum*, vol. 127, no. 3, pp. 507-518, May 2006.

[12] O. M. Grant, L. Tronina, H. G. Jones, and M. M. Chaves, “Exploring thermal imaging variables for the detection of stress responses in grapevine under different irrigation regimes.,” *Journal of Experimental Botany*, vol. 58, no. 4, pp. 815-25, Jan. 2007.

[13] L. Guilioni, H. Jones, I. Leinonen, and J. Lhomme, “On the relationships between stomatal resistance and leaf temperatures in thermography,” *Agricultural and Forest Meteorology*, vol. 148, no. 11, pp. 1908-1912, Oct. 2008.

[14] M. Fuchs, “Infrared measurement of canopy temperature and detection of plant water stress,” *Theoretical and Applied Climatology*, vol. 42, no. 4, pp. 253-261, 1990.

[15] M. Möller et al., “Use of thermal and visible imagery for estimating crop water status of irrigated grapevine.,” *Journal of experimental botany*, vol. 58, no. 4, pp. 827-38, Jan. 2007.

[16] I. Leinonen and H. G. Jones, “Combining thermal and visible imagery for estimating canopy temperature and identifying plant stress.,” *Journal of Experimental Botany*, vol. 55, no. 401, pp. 1423-31, Jun. 2004.

[17] M. Stoll and H. Jones, “Thermal imaging as a viable tool for monitoring plant stress,” *International Journal of Vine and Wine Sciences*, vol. 41, no. 2, pp. 77–84, 2007.

[18] E.-C. Oerke, R. Gerhards, and G. Menz, *Precision Crop Protection - The Challenge and Use of Heterogeneity*. Springer, 2010.

[19] L. Chaerle, W. V. Caeneghem, and E. Messens, “Presymptomatic visualization of plant-virus interactions by thermography,” *Nature*, vol. 17, no. 8, pp. 813-6, Aug. 1999.

[20] L. Chaerle, F. D. Boever, and M. Montagu, “Thermographic visualization of cell death in tobacco and Arabidopsis,” *Plant, Cell & Environment*, vol. 24, no. 1, pp. 15-25, Jan. 2001.

[21] L. Chaerle, I. Leinonen, H. G. Jones, and D. Van Der Straeten, “Monitoring and screening plant populations with combined thermal and chlorophyll fluorescence imaging.,” *Journal of Experimental Botany*, vol. 58, no. 4, pp. 773-84, Jan. 2007.

[22] E.-C. Oerke, U. Steiner, H.-W. Dehne, and M. Lindenthal, “Thermal imaging of cucumber leaves affected by downy mildew and environmental conditions.,” *Journal of Experimental Botany*, vol. 57, no. 9, pp. 2121-32, Jan. 2006.

[23] M. Lindenthal, U. Steiner, H.-W. Dehne, and E.-C. Oerke, “Effect of downy mildew development on transpiration of cucumber leaves visualized by digital infrared thermography.,” *Phytopathology*, vol. 95, no. 3, pp. 233-40, Mar. 2005.

[24] M. Stoll, H. Schultz, and B. Berkelmann-Loehnertz, “Thermal sensitivity of grapevine leaves affected by Plasmopara viticola and water stress,” *Vitis*, vol. 47, no. 2, pp. 133–134, 2008.

[25] H. G. Jones, R. Serraj, B. R. Loveys, L. Xiong, A. Wheaton, and A. H. Price, “Thermal infrared imaging of crop canopies for the remote diagnosis and quantification of plant responses to water stress in the field,” *Functional Plant Biology*, vol. 36, no. 11, p. 978, 2009.

[26] S. Merlot et al., “Use of infrared thermal imaging to isolate Arabidopsis mutants defective in stomatal regulation.,” *The Plant journal : for cell and molecular biology*, vol. 30, no. 5, pp. 601-9, Jun. 2002.

[27] J. Wardlaw, M. Gryka, F. Wanner, G. Brostow, and J. Kautz, “A New Approach to Thermal Imaging Visualisation: Thermal Imaging in 3D,” London, 2010.

[28] Y. Song, “Modelling and Analysis of Plant Image Data for Crop Growth Monitoring in Horticulture,” University of Warwick, 2009.

[29] D. Scharstein and R. Szeliski, “A taxonomy and evaluation of dense two-frame stereo correspondence algorithms,” *International journal of computer vision*, vol. 47, no. 1, pp. 7-42, 2002.

[30] H. Kim, “Hierarchical disparity estimation with energy-based regularization,” *Image Processing, 2003. ICIP 2003.*, pp. 5-8, 2003.

[31] P. Fua, “Combining stereo and monocular information to compute dense depth maps that preserve depth discontinuities,” *Proceedings of the 12th international joint conference*, pp. 1292-1298, 1991.

[32] S. Birchfield and C. Tomasi, “A pixel dissimilarity measure that is insensitive to image sampling,” *Pattern Analysis and Machine Intelligence, IEEE Transactions on*, vol. 20, no. 4, pp. 401-406, 1998.

[33] K. Konolige, “Small vision systems: Hardware and implementation,” *ROBOTICS RESEARCH-INTERNATIONAL*, 1998.

[34] R. Zabih and J. Woodfill, “Non-parametric local transforms for computing visual correspondence,” in *Computer Vision — ECCV ’94*, vol. 801, J.-O. Eklundh, Ed. Springer Berlin / Heidelberg, 1994, pp. 151-158.

[35] A. Klaus, M. Sormann, and K. Karner, “Segment-Based Stereo Matching Using Belief Propagation and a Self-Adapting Dissimilarity Measure,” *18th International Conference on Pattern Recognition (ICPR’06)*, pp. 15-18, 2006.

[36] J. Kim, V. Kolmogorov, and R. Zabih, “Visual correspondence using energy minimization and mutual information,” in *Proceedings Ninth IEEE International Conference on Computer Vision*, 2003, pp. 1033-1040 vol.2.

[37] H. Hirschmüller, “Accurate and efficient stereo processing by semi-global matching and mutual information,” *Vision and Pattern Recognition, 2005. CVPR*, vol. 2, pp. 807-814, 2005.

[38] H. Hirschmüller, “Stereo processing by semiglobal matching and mutual information.,” *IEEE transactions on pattern analysis and machine intelligence*, vol. 30, no. 2, pp. 328-41, Feb. 2008.

[39] H. Hirschmüller and D. Scharstein, “Evaluation of Cost Functions for Stereo Matching,” in *2007 IEEE Conference on Computer Vision and Pattern Recognition*, 2007, pp. 1-8.

[40] H. Hirschmüller and D. Scharstein, “Evaluation of stereo matching costs on images with radiometric differences.,” *IEEE transactions on pattern analysis and machine intelligence*, vol. 31, no. 9, pp. 1582-99, Sep. 2009.

[41] Y. Song, R. Wilson, R. Edmondson, and N. Parsons, “Surface Modelling of Plants from Stereo Images,” in *Sixth International Conference on 3-D Digital Imaging and Modeling (3DIM 2007)*, 2007, no. 3dim, pp. 312-319.

[42] N. R. Parsons, R. N. Edmondson, and Y. Song, “Image analysis and statistical modelling for measurement and quality assessment of ornamental horticulture crops in glasshouses,” *Biosystems Engineering*, vol. 104, no. 2, pp. 161-168, Oct. 2009.

[43] Y. Song, C. Glasbey, G. van der Heijden, and G. Polder, “Combining stereo and Time-of-Flight images with application to automatic plant phenotyping,” *Image Analysis*, vol. 1, pp. 467-478, 2011.

